

Mechanical Response of Caprine Muscle under Compression at Varying Strain Rates

Somnath H. Kadhane

Department of Mechanical Engineering,
Dr. B. A. Technological University,
Lonere-Raigad, India
shkadhane@gmail.com

Hemant N. Warhatkar

Department of Mechanical Engineering,
Dr. B. A. Technological University,
Lonere-Raigad, India
hnwarhatkar@dbatu.ac.in

Article Info

Volume 82

Page Number: 1245 - 1252

Publication Issue:

January-February 2020

Abstract

Soft tissues such as muscles in human body are subjected to varying strain rates under dynamic compressive loadings during automobile accidents. In contrast to recent safety tests involving crash dummies, an efficient method to predict the impact-induced injuries and risks is computational modelling and simulations. In high-impact scenario, development of an accurate human body model needs a thorough understanding of mechanical response of soft tissues at varying strain rates. In the present study, stress-strain response of caprine muscle tissue were tested under compressive loading at varying strain rates using custom-built polymeric split Hopkinson pressure bar (SHPB). Lower extremity muscle tissues were subjected to high strain rate compressive loadings at 600, 1700, 3200 and 4500 s⁻¹. The directional dependency of muscle tissue were examined along and perpendicular to muscle fiber direction. Caprine muscle tissue showed a non-linear and highly strain rate dependant mechanical response at high strain rates under compressive loading in both fiber directions. The experimental findings can further be used in the development of human body models of muscle tissues under impact loadings.

Keywords: SHPB; Strain rate; Soft tissue; Muscle; Compression; Stress-strain response.

Article History

Article Received: 14 March 2019

Revised: 27 May 2019

Accepted: 16 October 2019

Publication: 07 January 2020

I. INTRODUCTION

Soft tissues such as muscles, skin, brain, kidney and liver in human body are subjected to varying strain rates from low to high strain rate during dynamic loadings in various impact events such as automobile accidents, sports and recreation accidents, industrial accidents, ballistic impacts, blasts from explosions, slip and falls. Current advances in automobile crash simulations require fundamental and quantitative understanding of mechanical response of soft biological tissues in human body. As the mechanical response of most of

the soft tissues is dependent on strain rate, the mechanical response of soft biological tissues under dynamic loading is necessary to understand the injury patterns and mechanisms to develop the human body models, human-like dummies, safe and efficient body armors. The development of an accurate human body model needs extensive soft tissue properties and their high strain rate behavior beyond those already available in literature. Crash simulations with accurate finite element human body models would be the better predictors of injuries than with dummy models.

The low and intermediate strain-rate response of soft tissues has been characterized systematically using quasi-static and dynamic experimental setups [1-4]. SHPB originally developed by Hopkinson [5-6] and later improved by Kolsky [7] with two pressure bars connected in series has been widely used to characterize the dynamic behavior of ductile materials in the strain rate range of 10^2 - 10^4 s^{-1} [8]. The dynamic testing of soft tissues using SHPB with elastic bars may give inaccurate results due to the difficulties associated with dynamic stress-equilibrium, uniform deformation of specimen at constant strain rate and radial inertia effects in specimen [9]. The conventional SHPB can therefore be modified to obtain the mechanical response of soft biological tissues under compressive, tensile and torsional loading. A very few attempts have been invested to characterize the high strain-rate response of soft biological tissues. Recently, the SHPB with low impedance metallic bars has been used to investigate the mechanical response of soft tissues at varying strain rates. The SHPB setup uses long metallic bars such as aluminum and length of whole SHPB setup is few meters long. The stress-strain responses of bovine soft tissues such as kidney tissue [10], liver tissue [11], brain tissue [12]; porcine soft tissues such as liver tissue [13], adipose tissue [14], trachea tissue [15], lung tissue [16] have been recently studied over wide range of strain rates using modified versions of SHPB under compressive loading at varying strain rates. The mechanical response of porcine muscle [17] and bovine muscle [18] using low impedance metallic bars and PMHS muscle [19] and goat muscle [20] using polymeric bars has been studied systematically under compressive loading at varying strain rates. The stress-strain response of many soft tissues under dynamic loading is found to be very different than that of quasi-static response. The determination of attenuation coefficient in viscoelastic pressure bars using spectral analysis [21] and experimental incident bar tests [22] has been well demonstrated for the use of viscoelastic polymeric pressure bars in SHPB for the use of polymeric SHPB in the

dynamic characterization of soft tissues. Polymeric pressure bars was used in SHPB due the impedance matching with soft tissues for better wave transmission.

In the present work, SHPB has been successfully modified using polymeric pressure bars to study the mechanical response of caprine lower extremity muscle loaded along and perpendicular to the fiber direction under compressive loading at varying strain rates. The wave attenuation and dispersion correction has been incorporated in the viscoelastic analysis of polymeric SHPB using experimental method as suggested by Bacon [22]. The Labview assisted data acquisition system was used to acquire the stress waves propagating through the pressure bars during impact. Matlab program based on viscoelastic analysis of SHPB was used for dynamic characterization of muscle tissues. The experimental protocol to prepare the specimens from caprine muscles has been developed in-house.

II. VISCOELASTIC SHPB

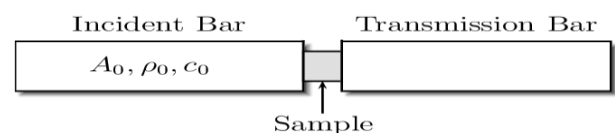


Figure 1. Schematic of Conventional SHPB

In recent years, the design developments and testing procedures in conventional SHPB have been well reviewed and documented [23]. The conventional SHPB as shown in figure 1 consists of three pressure bars viz; striker bar, incident bar and transmitter bar. A specimen is sandwiched between incident and transmitter bar. The impact of striker bar on the end of incident bar generates an elastic longitudinal strain pulse (incident pulse) propagating through the incident bar. At the specimen-incident bar interface, incident pulse splits and incident pulse is partly reflected back (reflected pulse) and partly transmitted (transmission pulse) into the transmitter bar. In elastic SHPB, it was assumed that the specimen is compressed between

incident and transmitter bar at dynamic stress equilibrium under constant strain rate. The reflected stress waves are used to calculate strain and the portion of compressive stress waves that continues through the specimen is used to calculate stress. One dimensional wave propagation theory in elastic pressure bars along axial direction yields the calculation of strain (ε_s), strain rate ($\dot{\varepsilon}_s$) and stress (σ_s) induced in the specimen using following equations.

$$\varepsilon_s = \frac{-2C_0}{L_s} \int_0^t \varepsilon_r dt \quad (1)$$

$$\dot{\varepsilon}_s = \frac{-2C_0}{L_s} \dot{\varepsilon}_r \quad (2)$$

$$\sigma_s = \frac{A_0}{A_s} E \varepsilon_t \quad (3)$$

Where, ε_r and ε_t are the reflected and transmitted strain histories, respectively; A_0 is the cross-sectional area of pressure bars; C_0 and E are the sound wave speed and modulus of elasticity in the pressure bar, respectively; A_s and L_s are the initial cross-sectional area and length of specimen, respectively.

If specimen is soft tissue, the dynamic stress equilibrium may not be achieved over entire loading duration due to low sound velocity of soft tissue. Polymeric pressure bars has been used to enable the low level stress signals propagating through pressure bars as the PMMA has closer impedance to the soft tissues. The uniform deformation of specimen at nearly constant strain rate under dynamic stress equilibrium can be achieved by using thin cylindrical specimen and PTFE pulse shaper. The analysis for the metallic SHPB is not directly applicable for polymeric SHPB bar. These bars are viscoelastic. The stress wave attenuates and disperses in the medium due to the use of polymeric bars in SHPB. The strain measured at the middle location of the pressure bar is different from the strain measured at the interface of bar-specimen. The attenuation and dispersion correction has to be applied to account the strain mismatch. The theory of one-dimensional stress-wave propagation along

axial direction and experimental procedure developed by Bacon (1998) is used to find the attenuation and the propagation coefficient in viscoelastic pressure bars. The reflected pulses were reconstructed using the attenuation and dispersion coefficients. The stress-wave equation of viscoelastic pressure bar is represented in the Fourier domain by

$$\frac{\partial \tilde{\sigma}_s(x, \omega)}{\partial x^2} = -\rho\omega^2 \tilde{\varepsilon}_s(x, \omega) \quad (4)$$

Where, $\tilde{\varepsilon}_s(x, \omega)$ and $\tilde{\sigma}_s(x, \omega)$ denote Fourier transformations of the longitudinal strain and normal stress, respectively. The frequency f is determined by $\omega=2\pi f$. The angular frequency, ω and frequency, f is represented in radians and Hz, respectively.

Neglecting lateral motion of the bars, the linear behavior of the polymeric bar can be given by the complex Young's modulus, $E^*(\omega)$ as follows

$$\tilde{\sigma}(x, \omega) = E^*(\omega) \tilde{\varepsilon}(x, \omega) \quad (5)$$

The wave propagation coefficient $\gamma(\omega)$, dependent on frequency in the polymeric bar is specified by

$$\gamma^2 = -\frac{\rho\omega^2}{E^*} \quad (6)$$

A general solution of one-dimensional wave equation along axial direction in the Fourier domain can be expressed by

$$\tilde{\varepsilon}_s(x, \omega) = \tilde{P}(\omega)e^{-\gamma x} + \tilde{N}(\omega)e^{\gamma x} \quad (7)$$

Where, $\tilde{N}(\omega)$ and $\tilde{P}(\omega)$ defines the Fourier transformations of the strains at $x = 0$ due to stress-wave propagation along decreasing and increasing x , respectively.

The wave propagation coefficient $\gamma(\omega)$, is the divided into two parts, viz real part $\alpha(\omega)$, and imaginary part $k(\omega)$.

$$\gamma(\omega) = \alpha(\omega) + ik(\omega) \quad (8)$$

The real part is the attenuation coefficient, and the imaginary part is the wave number. The wave number can be, the, used to determine the phase velocity.

The equations (9) and (10) represent the general solution and can be, further used to determine the Fourier transformations of force $\tilde{F}(x, \omega)$ as a function of frequency and velocity $\tilde{v}(x, \omega)$ as a function of position.

$$\tilde{v}(x, \omega) = -\frac{i\omega}{\gamma} \left[\tilde{P}(\omega)e^{-\gamma x} - \tilde{N}(\omega)e^{\gamma x} \right] \quad (9)$$

$$\tilde{F}(x, \omega) = -\frac{\rho A_0 \omega^2}{\gamma^2} \left[\tilde{P}(\omega)e^{-\gamma x} + \tilde{N}(\omega)e^{\gamma x} \right] \quad (10)$$

Lastly, the equations (9) and (10) are solved using inverse Fourier transforms, and used together with equations (2) and (3) to determine the stress-strain histories induced in the test specimen due the impact loading. Stress $\tilde{\sigma}_s(\omega)$, strain $\tilde{\epsilon}_s(\omega)$ and strain rate $\dot{\tilde{\epsilon}}_s(\omega)$ in the specimen are calculated using reconstructed waves in frequency domain.

$$\dot{\tilde{\epsilon}}_s(\omega) = -\frac{2 \tilde{\epsilon}_{R_new}(\omega)}{L_0} \left[\frac{i\omega}{\gamma(\omega)} \right] \quad (11)$$

$$\tilde{\epsilon}_s(\omega) = \int_0^t \dot{\tilde{\epsilon}}_s(\omega) dt \quad (12)$$

$$\tilde{\sigma}_s(\omega) = \frac{A_0 \tilde{\epsilon}_{T_new}(\omega)}{A_s} E^*(\omega) \quad (13)$$

Using inverse Fourier transform, stress $\sigma_s(t)$, strain $\epsilon_s(t)$ and strain rate $\dot{\epsilon}_s(t)$ in the specimen are then calculated in time domain.

III. EXPERIMENTAL SETUP

A. Sample Preparation

The caprine muscle was cut from the lower extremity of 10 Month old male goat immediately after it was slaughtered. The specimens were stored in saline solution at room temperature about 20°C for two hours before testing. All the specimens were thawed at room temperature for less than three hours before testing. The fascia layer was removed from the muscles. The dehydration of the muscle tissue is prevented during experimentation. The samples were cut into cylindrical specimens having diameter of 12 mm and length 3 mm using surgical scalpels. The length of the specimen which represents the

direction of loading was kept along and perpendicular to the fiber orientation of muscle tissue. The physical loading of muscle tissue was avoided till performing the tests.

B. Experimental Setup

The schematic of the polymeric SHPB setup used for the dynamic characterization of muscle under compressive loading is shown in figure 2. The incident and transmission bars of diameter 16 mm and length 1220 mm were made from polymeric material-PMMA. The solid striker bar made from PMMA having diameter 16 mm and length 400 mm has been used as projectile to obtain the compressive stress pulse after impacting it onto the incident bar. The cylindrical muscle specimen was sandwiched in between incident and transmitter bar with the help of petroleum jelly to avoid fall of specimen. The striker bar in gas operated launcher mechanism (not shown in figure) was accelerated forward against the incident bar by using quick acting solenoid valve.

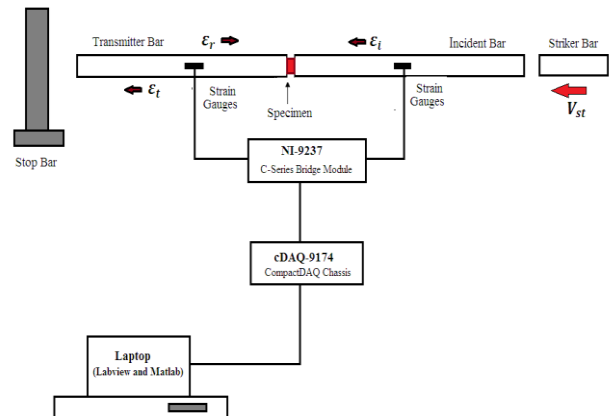


Figure 2. Schematic of Polymeric SHPB setup

Two pairs of foil type resistive strain gauges (Omega Engineering) were attached at the middle of both incident and transmitter bar to measure the incident and transmission waveform signals. PTFE disks were used as pulse shapers to obtain the dynamic stress equilibrium and to deform the specimen at nearly constant strain rate. The collision of striker bar on the end of incident bar creates the incident pulse (compressive) that propagates through the incident bar towards the specimen. The incident

pulse is recorded by the strain gauges mounted on the incident bar. Once the wave reaches to the specimen, it splits into two pulses viz. transmitted wave and reflected wave. The transmitted pulse (compressive) travels through the specimen and into the transmitter bar where the energy is recorded by the strain gauges mounted on transmitter bar. The second pulse (tensile) is reflected away from the specimen and travels back down to the incident bar. At the end of SHPB, a stop bar absorbs the impact of transmission bar to complete the test. The incident, reflected and transmitted stress pulses during compressive experiments on caprine muscle specimen at higher strain rates are shown in figure 3.

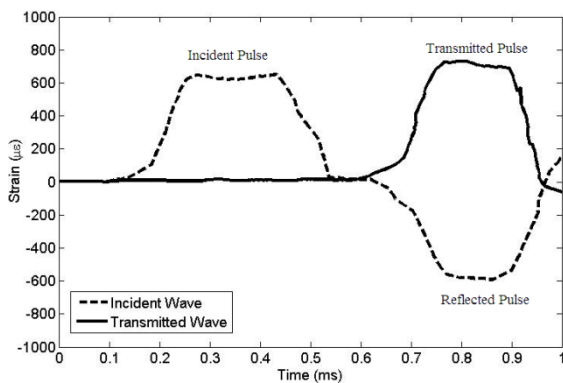


Figure 3. Waveform history obtained from polymeric SHPB experiment on a cylindrical caprine muscle specimen.

The frequency oscillations and initial spikes observed in measured stress pulses during experiments using elastic SHPB are nearly eliminated in viscoelastic SHPB tests due to use of pulse shaping and polymeric pressure bars. This facilitates accurate characterization of stress-strain response at higher strain rates under dynamic loading. The incident and reflected pulse are nearly same and opposite in sign due the mechanical impedance of the soft tissue is closer to the pressure bars. The transmitted pulse records the stress history and reflected pulse records the strain history in the specimen. Viscoelastic analysis of polymeric SHPB was used to determine the stress-strain response of muscle specimen using Matlab program.

C. Experimental Protocol

The only one test was conducted on each sample under unconfined condition. Each specimen is tested under compressive loading for the pressure range from 1 bar to 10 bars to obtain an average impact velocity of about 1 to 10 m/s. The muscle tissues were tested at strain rates of 600, 1700, 3200 and 4500 s^{-1} under compression loaded along and perpendicular to the muscle fiber directions. All the experimental tests were conducted at room temperature (20-25 °C). The only one test was conducted on each sample in unconfined condition. The tests were repeated at least 4 times at each strain rate under identical loading conditions to study the repeatability of experimental results.

D. Data Analysis

NI-LabVIEW assisted data acquisition system composed of NI 9237 bridge module and NIcDAQ 9174 chassis with LabVIEW 2014 software has been established to acquire and records the stress wave history using strain gauges mounted on the pressure bars. The incident and transmission bar signals were captured using incident and transmission strain gauges at 1 MHz for 2 milliseconds resulting in 2000 data points per test. A signal conditioning and amplification was done in programming using continuous sampling acquisition mode at sampling rate of 50 kHz. The waveform data has not been filtered during data acquisition; however this raw waveform data was filtered at 50 kHz for noise reduction using band pass filter. The signal to noise ratio (SN ratio) has been evaluated for the acquired waveforms and tests with SN ratio lower than 10 have been neglected for further analysis. The MATLAB program based on viscoelastic analysis was used to post process the recorded waveform. This enables the calculation of the propagation coefficient, reconstruction of the waveform at specimen-bar interface and determination of the stresses, strains and strain rates in the muscle specimen to plot the stress-strain response at each strain rate.

IV. RESULTS AND DISCUSSION

The average stress-strain responses of the caprine muscle are depicted in figure 4 and 5 for the compressive loading of the specimen along and perpendicular to the muscle fiber directions. Each muscle specimen was tested at five impact velocities corresponding to five strain rates from 600-4500 s⁻¹ up to failure. Each of the curves shown in these figures is the average of at least four repeated compressive experiments conducted at identical loading and testing conditions.

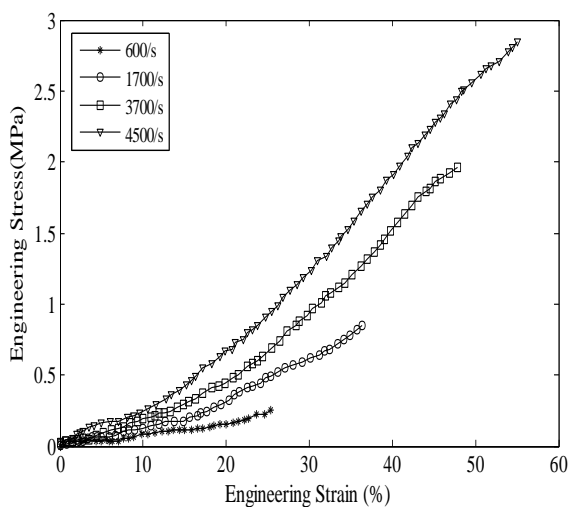


Figure 4. Stress-strain response of the caprine muscle along the fiber direction at various strain rates

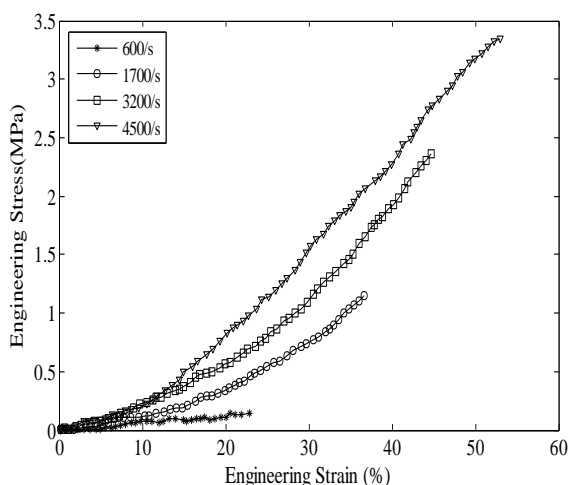


Figure 5. Stress-strain response of the caprine muscle perpendicular to the fiber direction at various strain rates

All stress-strain curves exhibit a toe region at the beginning, followed by a transitional non-linear

response and then a strain hardening response. This behavior is similar to those obtained previously in quasi-static experiments [1]. The comparison of stress-strain values at various strain rates is shown in table 1. The increase in applied strain rate leads to the increase in the work hardening effect of flow stresses.

TABLE I. COMPARISON OF STRESS-STRAIN VALUES AT VARIOUS STRAIN RATES OBSERVED IN CAPRINE MUSCLE ALONG AND PERPENDICULAR TO MUSCLE FIBER DIRECTION.

Strain Rate (s ⁻¹)	Strain (%)	Stress (MPa)	
		AL	TR
600	20	0.2	0.2
1700	30	0.6	0.7
3200	40	1.5	2.0
4500	50	2.5	3.2

At 50% strain, a maximum stress of 1.5 MPa and 2.0 MPa have been observed in caprine muscle loaded along and perpendicular to the fiber direction respectively at a strain rate of 3200 s⁻¹. Nie et al. [17] have reported a maximum stress of 0.3 MPa and 0.35 MPa at 30% strain for the porcine muscle loaded along and perpendicular to fiber direction at 2100 s⁻¹. Sligtenhorst et al. [18] conducted compressive testing of bovine muscle tissue by using SHPB at higher strain rates and reported a maximum stress of 2.4 MPa at 50% strain for the porcine muscle loaded along the fiber direction at 2300 s⁻¹. The stress-strain response of caprine muscle tissue is higher than that for porcine muscle tissue and lower than that for bovine muscle tissue. In the present study, stress-strain response of caprine muscle specimen has been found to be stiffer than porcine muscle response. As seen from figure 4 and 5, it was observed that the strain rate dependency is clearly sensitive to the loading direction. The strain rate sensitivity along the perpendicular direction is more significant than that along the fiber direction.

V. CONCLUSION

A polymeric SHPB setup has been designed and developed to establish an experimental procedure

for the characterization of impact response of muscle tissues at varying strain rates under dynamic compressive loading. The stress-strain behavior of goat muscles was investigated under dynamic compressive loading conditions at 600-4500 s⁻¹ and the stress-strain curve exhibits non-linear behavior under compressive dynamic loadings. The stress-strain response exhibits non-linear behavior under compressive dynamic loading and is strain-rate dependent. The muscle response obtained though the present study could further be used in finite element analysis. The maximum compressive stress and strain increases significantly with increase in strain rates. It is also observed that at the same strain rate, the specimen stress of caprine muscle along the fiber (TR) direction is higher than that along perpendicular fiber (AL) direction. It was also observed that the caprine muscle specimens along the fiber direction are stiffer than those from along the perpendicular fiber direction. The strain-rate dependent data will be used to formulate the constitutive material model to be used for muscle tissue modeling.

ACKNOWLEDGMENT

The authors express sincere thanks to DBATU, Lonere for providing the financial support to develop an SHPB experimental testing facility at DBATU, Lonere.

REFERENCES

- [1] Van L., Lyons, C., Simms, C., "Viscoelastic properties of passive skeletal muscle in compression: stress-relaxation behaviour and constitutive modeling," *Journal of Biomechanics*, 41: 1555-1566, 2008, doi: [10.1016/j.jbiomech.2008.02.007](https://doi.org/10.1016/j.jbiomech.2008.02.007)
- [2] Warhatkar, H., Chawla, A., Mukherjee, S., Malhotra, R., "Experimental Study of Variation between Quasi-Static and Dynamic Load Deformation Properties of Medial Collateral Knee Ligaments," *SAE World Congress, Detroit*, 2009, doi: [10.4271/2009-01-0392](https://doi.org/10.4271/2009-01-0392)
- [3] Zhai, X., Chen, W., "Compressive Mechanical Response of Porcine Muscle at Intermediate (10⁰/s-10²/s) Strain Rates," *Experimental Mechanics*, 2018, doi: [10.1007/s11340-018-00456-1](https://doi.org/10.1007/s11340-018-00456-1)
- [4] Zhai, X., Nauman, E., Nie, Y., Liao, H., et al., "Mechanical response of human muscle at intermediate strain rates," *Journal of Biomechanical Engineering*, 2019, doi: [10.1115/1.4042900](https://doi.org/10.1115/1.4042900)
- [5] Hopkinson, J., "Further experiments on the rupture of iron wire," Article 39, B. Hopkinson (ed.) (1872), *Original Papers-by the late John Hopkinson, Vol. II, Scientific Papers*, Cambridge, 1901, doi: [10.1098/rsta.2013.0220](https://doi.org/10.1098/rsta.2013.0220)
- [6] Hopkinson, B., "A Method of Measuring the Pressure Produced in the Detonation of High Explosives or by the Impact of Bullets," *Philosophical Transactions of the Royal Society of London: Series A*, 213: 437-456, 1914, doi: [10.1098/rspa.1914.0008](https://doi.org/10.1098/rspa.1914.0008)
- [7] Kolsky H., An investigation of the mechanical properties of materials at very high rates of loading, *Proceedings of the Physical Society-Section B* 62, (1949), 676-700, doi: [10.1088/0370-1301/62/11/302](https://doi.org/10.1088/0370-1301/62/11/302)
- [8] Davies, E., and Hunter, S., "The Dynamic Compression Testing of Solids by the Method of the Split Hopkinson Pressure Bar," *Journal of the Mechanics and Physics of Solids*, 11(3):155-179, 1963, doi: [10.1016/0022-5096\(63\)90050-4](https://doi.org/10.1016/0022-5096(63)90050-4).
- [9] Chen, W., "Experimental methods for characterizing dynamic response of soft materials," *Journal of Dynamic Behavior of Materials*, 2:2-14, 2016, doi: [10.1007/s40870-016-0047-5](https://doi.org/10.1007/s40870-016-0047-5).
- [10] Pervin, F., Chen, W., Weerasooriya, T., "Dynamic compressive response of renal cortex," *International Journal of Structural Changes in Solids*, 2(1):1-7, 2010, doi: [10.1115/IMECE2009-13180](https://doi.org/10.1115/IMECE2009-13180).
- [11] Pervin, F., Chen, W., Weerasooriya, T., "Dynamic compressive response of bovine liver tissue" *Journal of Mechanical Behaviour Biomedical Materials*, 4:76-84, 2011, doi: [10.1016/j.jmbbm.2010.09.007](https://doi.org/10.1016/j.jmbbm.2010.09.007).
- [12] Pervin, F., and Chen, W., "Dynamic mechanical response of bovine gray and white matter brain tissues under compression," *Journal of Biomechanics*, 42:731-735, 2009, doi: [10.1016/j.jbiomech.2009.01.023](https://doi.org/10.1016/j.jbiomech.2009.01.023).

- [13] Chen, J., Patnaik, S., Prabh, R., Proddy, L., et al., "Mechanical response of porcine liver tissue under high strain rate compression," *Biengineering*, 6(49):1-16, 2019, doi: [10.3390/bioengineering6020049](https://doi.org/10.3390/bioengineering6020049).
- [14] Comley, K., and Fleck, N., "The compressive response of porcine adipose tissue from low to high strain rate," *International Journal of Impact Engineering*, 46:1-10, 2012, doi: [10.1016/j.ijimpeng.2011.12.009](https://doi.org/10.1016/j.ijimpeng.2011.12.009).
- [15] Butler, B., Bo, C., Tucker, A., Jardine, A., et al., "Mechanical and histological characterization of trachea tissue subjected to blast-type pressures," *IOP Journal of Physics: Conference Series*, 18th APS-SCCM and 24th AIRAPT, 500, 2014, doi: [10.1088/1742-6596/500/18/182007](https://doi.org/10.1088/1742-6596/500/18/182007).
- [16] Sanborn, B., Nie, X., Chen, W., Weerasooriya, T., "High strain-rate pure shear and uniaxial compressive response of porcine lung tissue," *Journal of Applied Mechanics*, 80:11-29, 2013, doi: [10.1115/1.4007222](https://doi.org/10.1115/1.4007222).
- [17] Song, B., Chen, W., Ge Y., Weerasooriya, T., "Dynamic and quasi-static compressive response of porcine muscle," *Journal of Biomechanics*, 40 (2007), 2999-3005, doi: [10.1016/j.jbiomech.2007.02.001](https://doi.org/10.1016/j.jbiomech.2007.02.001)
- [18] Van, S. C., Cronin, D., Brodland, G., "High strain rate compressive properties of bovine muscle tissue determined using split Hopkinson bar apparatus," *Journal of Biomechanics*, 39:1852-1858, 2006, doi: [10.1016/j.jbiomech.2005.05.015](https://doi.org/10.1016/j.jbiomech.2005.05.015)
- [19] Karthikeyan, B., Mukherjee, S., Chawala, A., Malhotra, R., "Dynamic compressive response of passive human muscles using Split Hopkinson Pressure Bar," *Indian Journal of Biomechanics*, 1(3):20-28, 2012.
- [20] Kadhane, S., and Warhatkar, H., "Dynamic Stress-Strain Compressive Response of Soft Tissue using Polymeric Split Hopkinson Pressure Bar," *International Journal of Innovative Technology and Exploring Engineering*, 8(9):341-347, 2019.
- [21] Salisbury C., "Spectral analysis of wave propagation through a polymeric Hopkinson bar", MAS Thesis, Waterloo, Ontario-Canada, 2001.
- [22] Bacon, C., "An experimental method for considering dispersion and attenuation in a viscoelastic Hopkinson bar," *Experimental Mechanics*, 38:242-249, 1998, doi: [10.1007/BF02410385](https://doi.org/10.1007/BF02410385).
- [23] Davis R., "A critical study of the Hopkinson pressure bar," *Philosophical Transactions of the Royal Society of London: Series A*, 240: 375-457, 1948, doi: [10.1098/rsta.1948.0001](https://doi.org/10.1098/rsta.1948.0001).